

# Retrieving Filter Spectra in CNN for Explainable Sleep Stage Classification

Stephan Goerttler,<sup>1,2,\*</sup> Yucheng Wang,<sup>2</sup> Emadeldeen Eldele,<sup>3</sup> Fei He,<sup>1</sup> and Min Wu<sup>2</sup>

<sup>1</sup>Centre for Computational Science and Mathematical Modelling, Coventry University, Coventry CV1 2JH, UK

<sup>2</sup>Institute for Infocomm Research, Agency for Science, Technology and Research, 138632, Singapore

<sup>3</sup>Centre for Frontier AI Research, Agency for Science, Technology and Research, 138632, Singapore

Despite significant advances in deep learning-based sleep stage classification, the clinical adoption of automatic classification models remains slow. One key challenge is the lack of explainability, as many models function as black boxes with millions of parameters. In response, recent work has increasingly focussed on enhancing model explainability. This study contributes to these efforts by globally explaining spectral processing of individual EEG channels. Specifically, we introduce a method to retrieve the filter spectrum of low-level convolutional feature extraction and compare it with the classification-relevant spectral information in the data. We evaluate our approach on the MSA-CNN model using the ISRUC-S3 and Sleep-EDF-20 datasets. Our findings show that spectral processing plays a significant role in the lower frequency bands. In addition, comparing the correlation between filter spectrum and data-based spectral information with univariate performance indicates that the model naturally prioritises the most informative channels in a multimodal setting. We specify how these insights can be leveraged to enhance model performance. The code for the filter spectrum retrieval and its analysis is available at <https://github.com/sgoerttler/MSA-CNN>.

*Clinical relevance*— The proposed method adds to ongoing efforts toward model explainability in automatic sleep stage classification, which is a crucial factor for the clinical adoption of these models.

## I. INTRODUCTION

Sleep stage classification is essential for assessing sleep and diagnosing sleep disorders using polysomnography [1]. With advances in machine learning, deep learning-based sleep stage classification has garnered significant attention [2]. However, despite promising results, its clinical adoption remains limited due to challenges in validation, professional integration, and explainability [3].

Explainability is particularly crucial for regulatory compliance and building trust among clinicians and patients while advancing model development [4]. As a consequence, enhancing model explainability has gained significant traction in recent years. For instance, gradient-weighted class activation mapping has been used for post-hoc explanation of input importance [5, 6], as well as for highlighting weighted attention [7]. Furthermore, self-attention has been utilised to explain input importance [8] and even temporal interactions [9]. While these approaches demonstrate local, sample-specific explanations, global explainability methods, such as surrogate ablation techniques, have been used to assess the contribution of individual modalities [10].

This work aims to extend existing efforts by introducing a method for explaining spectral information processing in a multivariate context. Our approach can be applied to classification models that leverage temporal convolutional feature extraction. In particular, our method retrieves the frequency spectrum of filters in the initial

convolutional layer. As this layer often comprises several pathways to cover the multiple spectral scales relevant in neurophysiology [9, 11], we introduce a unification assignment matrix to integrate these pathways. Further, we correlate the extracted filter spectrum with the classification-relevant spectral information in the data, which provides insight into the extent of spectral information processing. Lastly, we compare these correlations with the single-channel performance.

We evaluate the proposed method on two datasets using our previously introduced Multi-Scale and Attention Convolutional Neural Network (MSA-CNN), which is well-suited for analysing a broad spectral range (0-46.7 Hz).

## II. METHODOLOGY

### A. Method Overview

An overview of our proposed method, applied to the MSA-CNN [9], is presented in Fig. 1. The principal idea is to explain channel-wise spectral processing within the first convolutional feature extraction layer. In the MSA-CNN, this layer consists of four multi-scale convolutions. The filters of these convolutions capture distinct frequencies, which are given by their Fourier transform as well as their scale. We unify the frequencies across the scales using an assignment matrix  $\mathbf{S}_{\text{unif}}$ . The final filter spectrum is then compared with the between-class spectral variation in the data, which serves as an indicator of classification-relevant spectral information.

---

\* Stephan Goerttler (goerttlers@uni.coventry.ac.uk) is supported by the A\*STAR Research Attachment Program (ARAP).

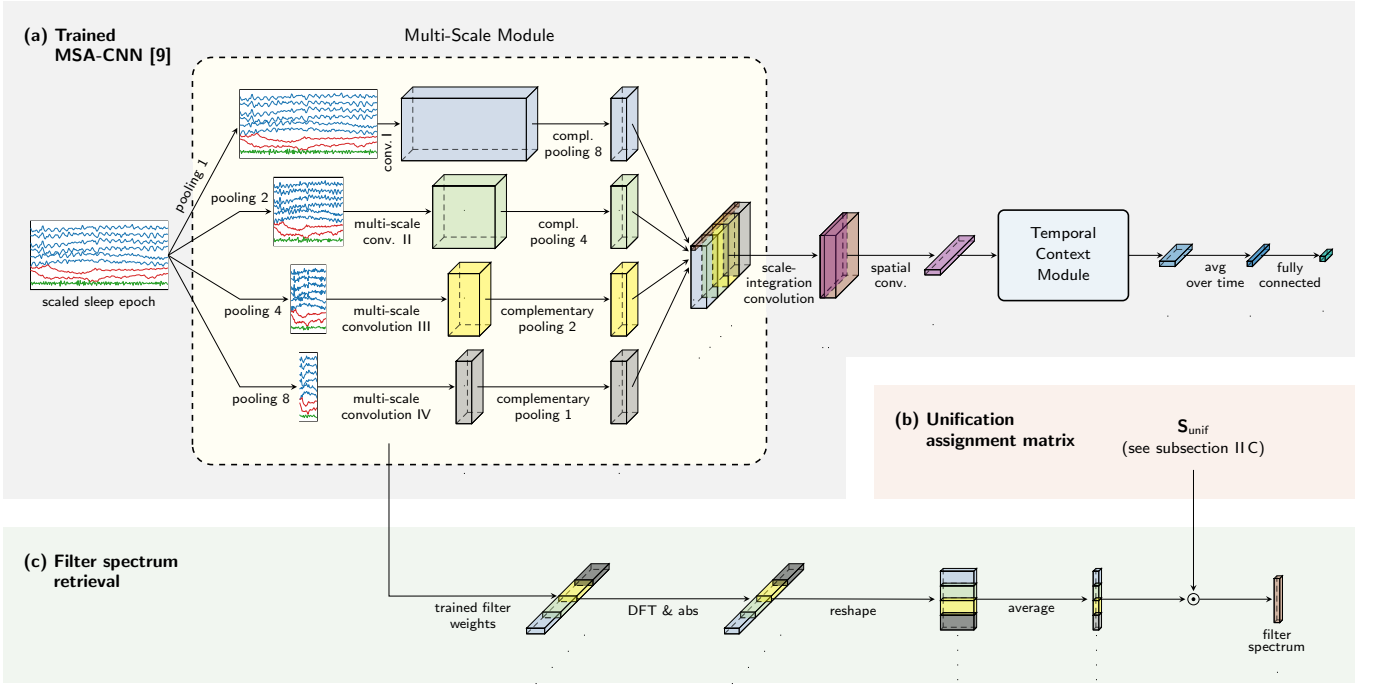


FIG. 1: Overview of proposed filter spectrum retrieval model with multi-scale convolution. (a) Trained MSA-CNN model on which the proposed method is tested. The trained weights of the first convolutional layer, comprising four multi-scale convolutions, are used to retrieve the filter spectrum. (b) Computation of unification assignment matrix  $\mathbf{S}_{\text{unif}}$ , using the pooling values of the multi-scale convolution. The matrix transforms scale-based frequency to unified frequency. (c) The trained filter weights are Fourier-transformed, reshaped, and averaged. Multiplication with  $\mathbf{S}_{\text{unif}}$  yields the final filter spectrum.

## B. Multi-Scale and Attention Convolutional Neural Network (MSA-CNN)

This study tests spectral processing in the MSA-CNN [9], which is shown in Fig. 1 (a). To begin with, a multi-scale convolution and a scale-integration convolution, which together form the Multi-Scale Module, extract spectral features for each channel. Subsequently, the channels are combined using a global spatial convolution. The time-resolved features are then passed to an attention-based Temporal Context Module (TCM), which captures long-range temporal dependencies. The TCM combines multi-head attention with a feed-forward neural network (for more details regarding the TCM, see [9]). Finally, the resulting features are averaged over time and interpreted using a fully connected layer.

## C. Unification Assignment Matrix

In deep learning-based neurophysiology models, the first convolutional layer typically comprises convolutions on multiple scales. This requires the use of a unification assignment matrix  $\mathbf{S}_{\text{unif}}$ , which assigns the scale-based frequencies to unified frequencies on a single scale.

The scale-based frequencies are collected in the list

$\mathbf{f}_{\text{sc}} = (f_0^{(I)}, f_1^{(I)}, \dots, f_0^{(II)}, \dots, f_{[N_t/2]}^{(IV)})$ . We determine the list of unified frequencies  $\mathbf{f}_{\text{unif}}$  by sorting  $\mathbf{f}_{\text{sc}}$  by magnitude and removing duplicate frequencies. The unnormalised assignment matrix is then given by:

$$\hat{\mathbf{S}}_{\text{unif},ij} = \begin{cases} 1, & \text{if } \mathbf{f}_{\text{unif}}[i] = \mathbf{f}_{\text{sc}}[j], \\ 0, & \text{otherwise.} \end{cases} \quad (1)$$

The matrix is then normalised using the diagonal matrix  $\mathbf{D}_{ii} = \sum_j \hat{\mathbf{S}}_{\text{unif},ij}$ , which finally yields  $\mathbf{S}_{\text{unif}} = \mathbf{D}^{-1} \hat{\mathbf{S}}_{\text{unif}}$ .

## D. Filter Spectrum Retrieval

The filter spectrum retrieval is illustrated in Fig. 1 (c). Firstly, the filter weights of the first convolutional layer are extracted from the trained model. Note that the layer can be either unimodal, where a single set of filters is trained and shared across all channels, or multimodal, where a separate set of filters is trained for each channel and modality. Secondly, the discrete Fourier transform (DFT) is applied to the filter weights. Only positive frequencies and magnitudes are kept for further processing. Thirdly, the resulting feature maps are reshaped and averaged, producing the filter spectrum in terms of scale-based frequencies. Finally, the filter spectrum is multi-

plied by the assignment matrix  $\mathbf{S}_{\text{unif}}$  to unify the scales of the convolutional layer, if required.

### E. Between-Class Spectral Variation

The goal of this subsection is to assess the spectral information relevant for classification for each channel. To this end, we introduce the between-class spectral variation, which quantifies spectral density variation between class means normalised by within-class variation. Specifically, we compute the spectral density as the square root of Welch’s power spectral density for every time series. The between-class variation is then retrieved by firstly averaging the spectral density across all samples for each class, and subsequently computing the standard deviation between the classes. On the other hand, the within-class variation is retrieved by computing the standard deviation for each class before averaging across all classes. Lastly, we divide the between-class variation by the within-class variation to obtain our final measure of relevant spectral information.

## III. EXPERIMENTS

### A. Datasets

We use the publicly available datasets ISRUC-S3 and Sleep-EDF-20 in this study. The **ISRUC-S3** was recorded by Khalighi et al. from 10 healthy subjects during sleep [12]. The recordings were divided into 30-second epochs and labelled, resulting in a total of 8,589 annotated samples. For our experiment, we only use channels with sufficient spectral structure, which includes the six referenced electroencephalography (EEG) channels, the two electrooculography (EOG) channels, and the electromyogram (EMG) channel. The input signals are downsampled to 100 Hz and preprocessed with a fourth-order low-pass Butterworth filter at 40 Hz cutoff frequency.

The **Sleep-EDF-20** dataset is sourced from PhysioBank [13]. The dataset comprises 20 subjects and has overall 42,308 labelled, artefact-free 30-second samples with a sampling rate of 100 Hz. Channels with spectral structure include two referenced EEG channels (Fpz-Cz and Pz-Oz) and the EOG channel. Similarly to the ISRUC-S3 dataset, we preprocessed the data with a 40 Hz low-pass filter.

### B. Model Training and Single-Channel Performance

The model parameters for all configurations are listed in Table I. Both temporal convolutional layers are set to unimodal, meaning that filters are shared across channels. We tailored the model size to each dataset, using a

TABLE I: Model parameters for MSA-CNN small and MSA-CNN large, based on multivariate or univariate inputs. Kernel sizes are specified by their spatial and temporal dimensions

layer	hyperparameter	MSA-CNN (small)		MSA-CNN (large)	
		multivar.	univar.	multivar.	univar.
MSM I	# scales	4		4	
	filter size	1×15		1×15	
	# filters / scale	8		8	
MSM II	filter size	1×5		1×5	
	# filters	16		32	
spatial	filter size	$N_{ch} \times 1$	$1 \times 5$	$N_{ch} \times 1$	$1 \times 5$
	# filters	32		64	
TCM	embedding dim.	16		32	
	# heads	2		4	
	# layers	1		2	

small configuration for ISRUC-S3 and a large configuration for Sleep-EDF-20. All models were trained for 100 epochs using the Adam optimizer [14], with a learning rate of 0.001 and a batch size of 64. Regularisation was applied using a dropout rate of 0.1 and weight decay of 0.0001. Multivariate models were trained on the entire dataset, while univariate models were trained and evaluated using 10-fold cross-validation, with performance measured as mean accuracy.

### C. Filter Spectrum vs. Between-Class Variation

To test our method, we retrieve the filter spectra for the multivariate models trained on both datasets and compare it to the between-class variation of each channel. Given the unimodal setting of our model, only one filter spectrum is retrieved for each dataset. The unification assignment matrix was computed using the pooling settings shown in Fig. 1(a) as well as the filter size setting of 15. Based on the sampling rate of 100 Hz, the unified frequencies span the range 0-46.7 Hz with a maximal frequency spacing of 6.7 Hz. Fig. 2 shows the filter spectrum for both datasets, overlaid with the respective between-class variation spectra of the frontal EEG channels F3-A2 (ISRUC-S3) and Fpz-Cz (Sleep-EDF-20). All spectra were rescaled by dividing by standard deviation. On both datasets, the results indicate substantial similarity between filter spectrum and between-class variation in the lower frequency bands alpha, theta and delta. This result indicates that the model uses mainly lower frequencies for spectral information-based classification. On the other hand, the filter spectra align across datasets in the higher frequency bands beta and gamma, which suggests that higher frequencies may be used to construct complex wave patterns shared across EEG datasets.

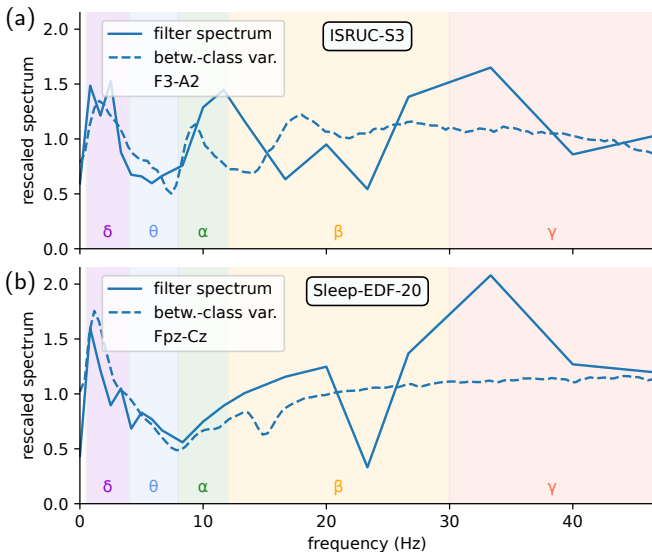


FIG. 2: Rescaled filter spectrum of datasets ISRUC-S3 (a) and Sleep-EDF-20 (b), overlaid with the rescaled between-class variation for the respective frontal channels F3-A2 and Fpz-Cz. At lower frequency bands alpha, theta and delta, filter spectra and between-class variations align.

#### D. Spectral Information Extraction Relative to Modality

To understand the specific role of channel and modality in extracting spectral information, we compute the Pearson correlation of filter spectrum and between-class variation across channels, as shown in Fig. 3 (a,b). We find that the correlation is highest for EEG (blue), followed by EOG (red) and EMG (green). This pattern is less pronounced for the ISRUC-S3 dataset, where EOG channels correlate almost as strongly with filter spectrum as EEG channels. There is also a within-modality discrepancy between frontal and occipital EEG channels: While for ISRUC-S3, frontal (blue) and occipital (light blue) channels correlate equally with filter spectrum, for Sleep-EDF-20 occipital channels correlate stronger than frontal channels. We validate these results by comparing them to the univariate performance achievable with the respective channel and modality. The univariate performances, shown in Fig. 3 (c,d), exhibit a similar pattern, with EEG outperforming EOG and EMG. This matching between correlation and performance indicates that the model is capable of prioritising more informative channels by optimising the retrieval of spectral information for these channels. Given the unimodal setting of the model, this prioritisation comes at the cost of neglecting less informative modalities.

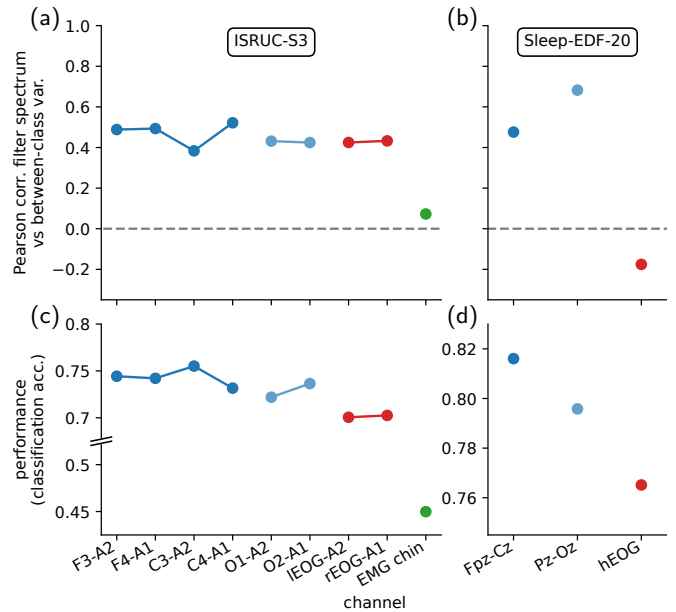


FIG. 3: (a,b) Channel-wise Pearson correlation between spectral activation and between-class variation for datasets ISRUC-S3 (a) and Sleep-EDF-20 (b). Generally, EEG channels (blue) exhibit the highest similarity, followed by EOG (red) and EMG (green). (c,d) Channel-wise classification performance for the two respective datasets. Channel performance approximately matches the correlations in (a,b).

#### IV. CONCLUSION

This study explored the role of spectral information processing for sleep stage classification in a multimodal setting. To begin with, we found that the filter spectrum aligns with the spectral information in the data at lower frequencies, thereby optimising spectral information extraction at these frequencies. This result highlights the way in which convolutional layers can function as spectral feature extractors [15]. At higher frequencies, filter spectrum and data-based spectral information diverge, while filter spectra align across datasets. This suggests that the filters capture the general morphology of EEG waves rather than spectral information at these frequencies. The capability to capture both spectral and morphological features is in contrast to spectral density extractors such as Welch’s method, which are limited to spectral features.

We further found that the model prioritises the most informative channels at the expense of less informative ones. Apart from providing insight into model functioning, this finding may be leveraged for performance optimisation in the following ways: First, channel selection for single- and multi-channel applications can be performed with only a single trained multivariate model. Second, comparisons between filter spectrum and between-class variation can be used to balance the fre-

quency scales for optimal spectral information extraction. Third, large discrepancies in between-class variation can signal the need for multimodal feature extraction. Together, these examples underscore the value of

our method for model improvement specifically, and the value of explainability for healthcare applications more generally.

- 
- [1] J. V. Rundo and R. Downey III, "Polysomnography," *Handbook of clinical neurology*, vol. 160, pp. 381–392, 2019.
- [2] X. Zhang, X. Zhang, Q. Huang, Y. Lv, and F. Chen, "A review of automated sleep stage based on eeg signals," *Biocybernetics and Biomedical Engineering*, 2024.
- [3] H. Yue, Z. Chen, W. Guo, L. Sun, Y. Dai, Y. Wang, W. Ma, X. Fan, W. Wen, and W. Lei, "Research and application of deep learning-based sleep staging: Data, modeling, validation, and clinical practice," *Sleep Medicine Reviews*, p. 101897, 2024.
- [4] K. Rasheed, A. Qayyum, M. Ghaly, A. Al-Fuqaha, A. Razi, and J. Qadir, "Explainable, trustworthy, and ethical machine learning for healthcare: A survey," *Computers in Biology and Medicine*, vol. 149, p. 106043, 2022.
- [5] F. Vaquerizo-Villar, G. C. Gutiérrez-Tobal, E. Calvo, D. Álvarez, L. Kheirandish-Gozal, F. Del Campo, D. Gozal, and R. Hornero, "An explainable deep-learning model to stage sleep states in children and propose novel eeg-related patterns in sleep apnea," *Computers in Biology and Medicine*, vol. 165, p. 107419, 2023.
- [6] M. Dutt, S. Redhu, M. Goodwin, and C. W. Omlin, "Sleepxai: An explainable deep learning approach for multi-class sleep stage identification," *Applied Intelligence*, vol. 53, no. 13, pp. 16 830–16 843, 2023.
- [7] G. Liu, G. Wei, S. Sun, D. Mao, J. Zhang, D. Zhao, X. Tian, X. Wang, and N. Chen, "Micro sleepnet: efficient deep learning model for mobile terminal real-time sleep staging," *Frontiers in Neuroscience*, vol. 17, p. 1218072, 2023.
- [8] B. Adey, A. Habib, and C. Karmakar, "Exploration of an intrinsically explainable self-attention based model for prototype generation on single-channel eeg sleep stage classification," *Scientific Reports*, vol. 14, no. 1, p. 27612, 2024.
- [9] S. Goerttler, Y. Wang, E. Eldele, M. Wu, and F. He, "Msa-cnn: A lightweight multi-scale cnn with attention for sleep stage classification," 2025. [Online]. Available: <https://arxiv.org/abs/2501.02949>
- [10] C. A. Ellis, R. Zhang, D. A. Carbajal, R. L. Miller, V. D. Calhoun, and M. D. Wang, "Explainable sleep stage classification with multimodal electrophysiology time-series," in *2021 43rd Annual International Conference of the IEEE Engineering in Medicine & Biology Society (EMBC)*. IEEE, 2021, pp. 2363–2366.
- [11] A. Supratak, H. Dong, C. Wu, and Y. Guo, "Deepsleepnet: A model for automatic sleep stage scoring based on raw single-channel eeg," *IEEE Transactions on Neural Systems and Rehabilitation Engineering*, vol. 25, no. 11, pp. 1998–2008, 2017.
- [12] S. Khalighi, T. Sousa, J. M. Santos, and U. Nunes, "Isruc-sleep: A comprehensive public dataset for sleep researchers," *Computer methods and programs in biomedicine*, vol. 124, pp. 180–192, 2016.
- [13] A. L. Goldberger, L. A. Amaral, L. Glass, J. M. Hausdorff, P. C. Ivanov, R. G. Mark, J. E. Mietus, G. B. Moody, C.-K. Peng, and H. E. Stanley, "Physiobank, physiotoolkit, and physionet: components of a new research resource for complex physiologic signals," *circulation*, vol. 101, no. 23, pp. e215–e220, 2000.
- [14] D. P. Kingma, "Adam: A method for stochastic optimization," *arXiv preprint arXiv:1412.6980*, 2014.
- [15] O. Rippel, J. Snoek, and R. P. Adams, "Spectral representations for convolutional neural networks," *Advances in neural information processing systems*, vol. 28, 2015.